



## Revolutionising Smart Home Energy Management: Advanced Integration of Solar Photovoltaics and E-Vehicles

**K.Gowtham,**

Research scholar, Department of electrical and electronics engineering.

Dr.M.G.R Educational and research institute, Chennai.

**Dr.M. Kumaresan,**

Department of electronics and communication engineering,

Dr.M.G.R Educational and research institute, Chennai.

### Abstract

The urgent need to mitigate environmental pollution and decrease fuel dependency has driven the development of renewable energy technologies and electric vehicles (EVs). However, integrating these into the power grid poses challenges due to production instability and irregular charging patterns. This study proposes an innovative energy management strategy for smart homes equipped with both EVs and photovoltaic (PV) systems. Utilizing a two-stage monitoring system, the strategy flexibly controls energy flow to minimize electricity costs and align with load curves while meeting power requirements. Results demonstrate distinct efficiencies among scenarios, with Case 2 exhibiting the best performance, followed by Case 3 and Case 1. Notably, integrating PV systems significantly reduces energy expenses, with savings ranging from \$2.30 to \$2.42 across cases. The study underscores the effectiveness of PV technology in residential energy management, emphasizing substantial cost reductions and decreased grid dependency. Through strategic battery usage and optimized PV energy utilization, the integration of renewable energy and EVs offers a promising pathway towards sustainable and resilient energy systems in smart homes.

**Keywords:** Electric vehicles (EVs); Energy management strategy; Photovoltaic (PV) systems; Cost optimization; SC-GWO

### 1. Introduction

Global issues of great concern now include the depletion of fossil resources and the rising pollution of the environment from the electricity and transportation industries [1,2]. As a result, the power and transportation sectors, respectively, have been driving the development of renewable energy technologies and electric vehicles (EVs) due to the pressing need to reduce fuel reliance and alleviate environmental pollution [3-5]. On the other hand, demand peaks, voltage variations, high load variability, and over-generation can all arise in the power grid as



a result of the inherent production instability of renewable energy sources like wind power and solar photovoltaics paired with the irregular charging patterns of EVs [6,7]. In order to overcome these obstacles, efficient energy management is needed to balance renewable energy production with EV charging schedules [8,9]. In light of this, current research has concentrated on developing efficient energy management systems to incorporate EVs and renewable energy sources into houses and the electrical grid. The notion of the smart grid, in conjunction with the bi-directional communication technology offered by smart meters, has brought forth a plethora of benefits and prospects, including financial incentives and enhanced energy efficiency. Moreover, home energy management systems (HEMS) and improvements in home area networks (HAN) and the smart grid environment enable homeowners to regulate generation, storage, and consumption [10–12]. In order to satisfy energy requirements while lowering household power expenditures and grid stress, HEMS automatically schedules EVs, distributed domestic energy resources, and household appliances based on time-varying pricing [12–14].

Researchers have recently paid close attention to HEMS combined with EVs, with certain studies emphasizing cost reduction [15, 16]. By analyzing the charging and discharging strategy of EVs in HEMS, for example, research in [15] investigated the economic benefits of different operating modes under dynamic pricing schemes, such as vehicle-to-grid (V2G), vehicle-to-home (V2H), and grid-to-vehicle (G2V). In order to minimize power expenditures while meeting EV charging and household energy demands, the authors of [16] suggested stochastic dynamic programming for optimum energy management in a smart home outfitted with an EV. This method defined the various operation modes (G2V, V2G, and V2H) using the time-varying home power demand and electricity price. It then formulated the stochastic optimization problem for EV energy management in a smart home using the EV battery equivalent circuit and probabilistic trip length and time. Flattening the load power profile has been the focus of several investigations [17, 18]. In order to flatten the load curve and reduce load variation, for instance, [17] presented a flexible control strategy for a smart home with two EVs. This was achieved without the use of time-varying electricity prices by monitoring the system in various operation modes based on constraints such as the daily power load curve of household appliances, EV connection time, state of charge (SOC) of each vehicle battery, and vehicle priority order. In order to smooth the load demand profile in a smart house with EVs and appliances, a double-layer energy management technique was presented in [18]. While the second layer controlled bidirectional power flow among EVs and the smart grid to schedule EV charging and discharging, it did not use the time-varying price, potentially increasing home electricity costs. The first layer used the power load curve and time-varying electricity price to shift appliance use from peak to off-peak hours. Reducing home expenses and grid stress has been the focus of several investigations [19]. For example, in order to reduce household power costs and grid interference, [19] developed a heuristic technique to determine



the best times of day to charge or discharge the EV battery based on household demand, real-time pricing signals, and EV specifications.

Along with PV and EV, HEMS integration has also been the subject of several research [20–23]. A HEMS utilizing a mixed-integer linear programming (MILP) approach was suggested in [20] for a smart house that included energy storage systems (ESS), EVs, and small-scale distributed photovoltaics in order to save daily power expenses. With a PV array and an EV for energy storage, the authors of [21] suggested a stochastic optimization-based energy management control for a smart home. This control would minimize customer energy costs while satisfying domestic power demands and EV battery charging goals. To reduce total energy expenditures while satisfying the needs of charging storage devices and meeting household power demands, a study [22] recommended coordinated energy management for a smart house equipped with PV, EVs, and home battery storage based on an energy price tag (EPT). In order to save power bills, [23] also presented a hierarchical deep reinforcement learning strategy for energy management in a smart house outfitted with EVs, electrical appliances, ESS, and a rooftop solar system.

Taking into account the noteworthy contributions of the previously stated research, it is clear that the integration of electric vehicles (EVs) and solar (PV) systems with home energy management systems (HEMS) has mainly targeted energy cost reduction. While some research focus just on the daily home load curve, others try to flatten the load curve by charging EVs during low-demand periods and discharging them during peak demand times. These methods, however, frequently ignore the seasonal fluctuations in power rates, which might result in increased family energy expenses.

Considering this, it is imperative to create a novel energy management plan for smart houses that have PV and EV systems installed. This strategy's main goal is to flexibly manage the energy flow to and from the EV in order to fulfill the system's power requirements, decrease electricity costs, and align with the load curve. This study's distinctive feature is its two-stage monitoring system, which is triggered in different ways according to different parameters: daily PV power generation profile, real-time price signals, daily power load curve for home appliances, EV arrival and departure times, and preserving the EV battery's state of charge (SOC).

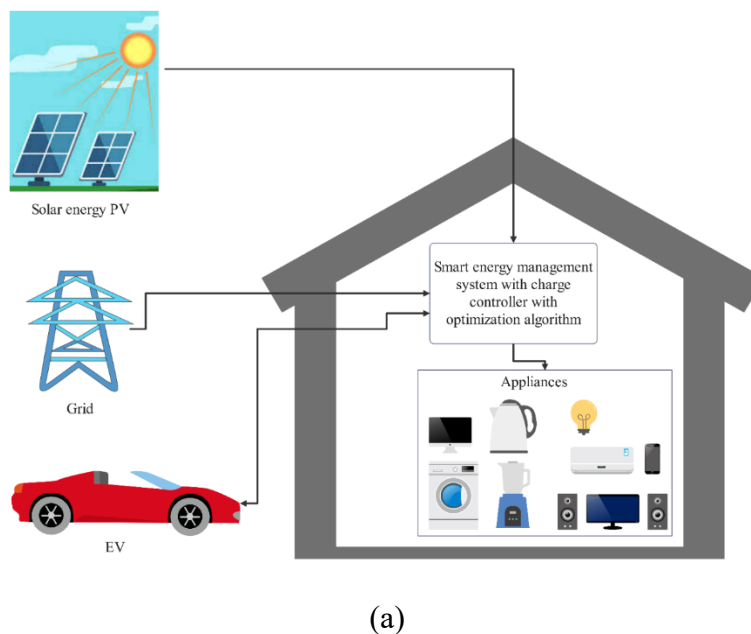
The suggested method is adaptable and works with any house that has EV and PV systems installed. By charging the EV from the grid and PV power when energy costs and consumption are low and PV generation exceeds the household load, it provides homeowners with financial benefits while also supporting the residential grid. During peak hours, peak energy from PV and the grid may be used to power the EV battery. This paper investigates the home energy management system (HEMS) as an essential tool for lowering electricity expenses. The objective is to identify the optimal architecture that reduces energy costs while satisfying the



demands of both home and EV loads, and keeping the state of charge (SOC) of the battery bank at the desired level. The SC-GWO algorithm is employed to achieve optimal energy scheduling and minimize the overall cost. The study evaluates three different scenarios, referred to as case 1, case 2, and case 3, for two distinct conditions: with photovoltaic (PV) integration and without PV.

## 2. Methodology

This study delves into three distinct scenarios aimed at determining the optimal architecture for minimizing energy costs while simultaneously fulfilling home and EV load requirements, all while ensuring the desired state of charge (SOC) for the battery bank. To achieve this goal, SC-GWO has been employed individually to assess and identify the most efficient design scenario in terms of energy cost reduction and SOC maintenance. The entire programming implementation was carried out using the Python programming language. The study's schematic diagram, depicted in the accompanying Fig 1 (a-b), visually outlines the systematic process undertaken in this research. Fig 2 (a-b). serves as a comprehensive representation of the methodologies employed, illustrating how the algorithms, load predictions, battery charging and discharging strategies, and energy distribution mechanisms all interplay to optimize energy consumption patterns. The study places special emphasis on maintaining the battery bank's SOC at the desired level, ensuring its effective usage during peak energy demand scenarios. Through this multifaceted approach, the study advances our understanding of effective energy management strategies that simultaneously balance cost savings and operational efficiency.



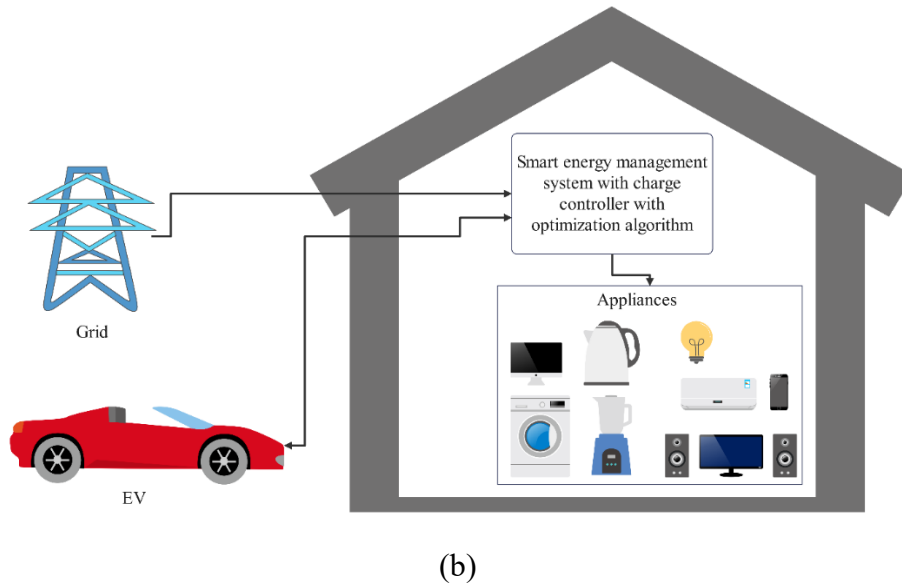
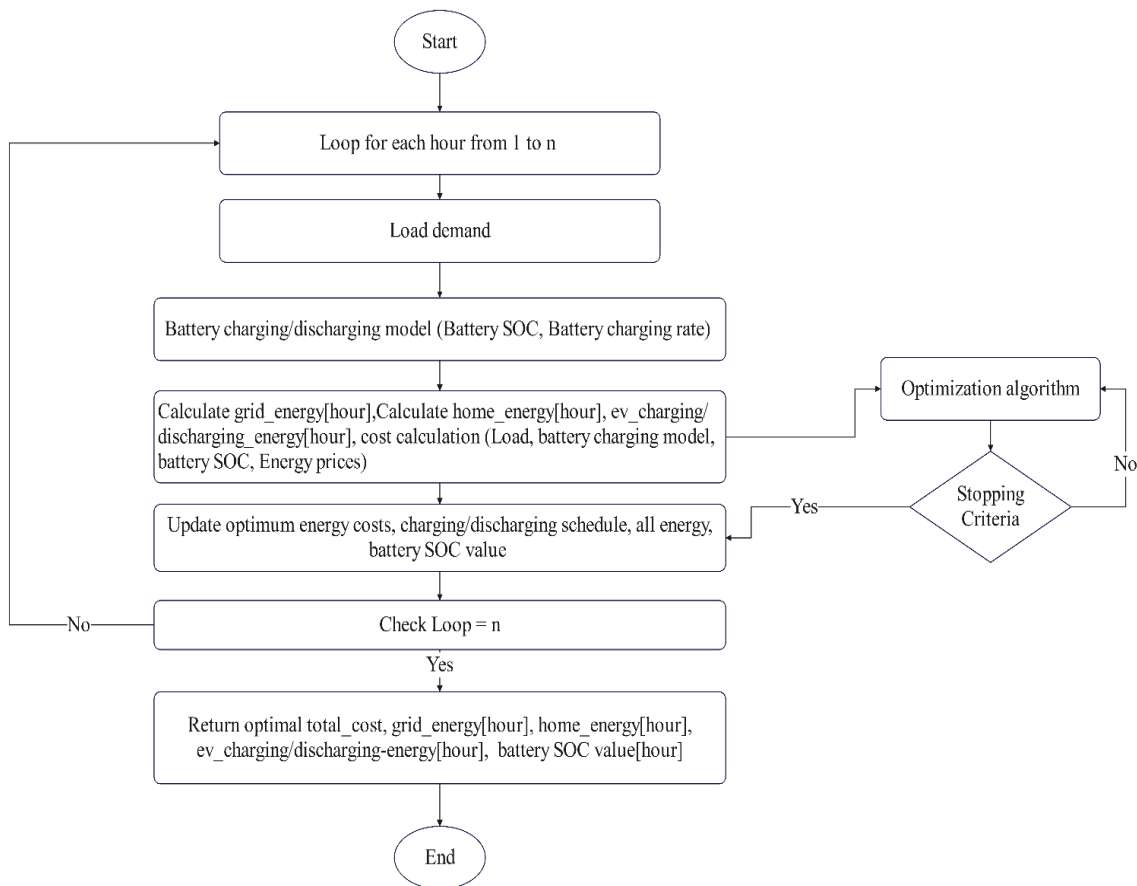
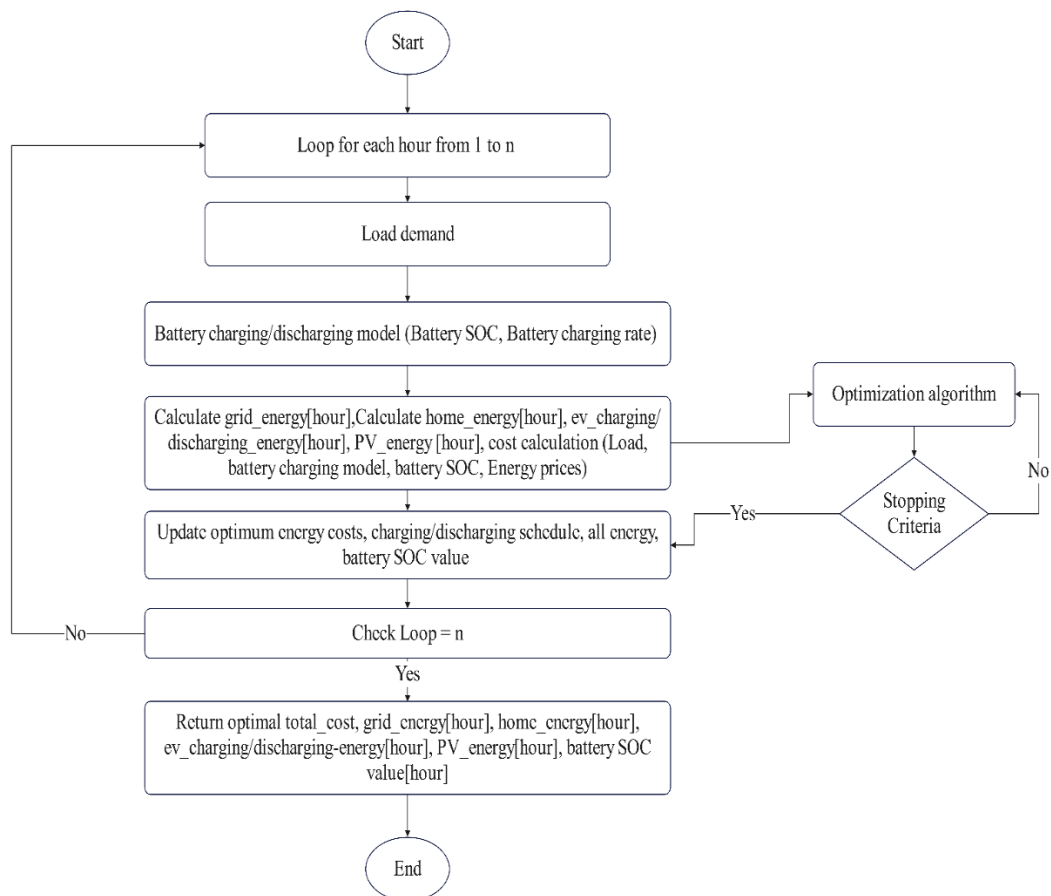


Fig 1. Schematic diagram of the proposed model (a) with PV (b) without PV



(a) Without PV integration



(b) With PV integration

Fig 2. Flow diagram of the proposed model

To discover the most efficient charging/discharging timetables for the electric vehicle battery array, aiming to reduce energy expenses while upholding the battery bank's state of charge at 0.9, two distinct optimization methods have been employed. One approach involves a linear algorithm, while the other utilizes a genetic algorithm. These algorithms have been harnessed to design and find the optimum structure of a Home Energy Management System, which orchestrates the power distribution among the grid, EV battery bank, and household consumption.

### Case 1:

This case has been examined under two conditions: one with PV and one without PV. In this scenario, the initial power is allocated to both the household and the electric vehicle (EV) simultaneously, sourced from both PV and the grid. During periods of peak energy demand, the stored energy from the EV battery bank and PV attempts to meet the demand with minimal use of grid energy. Throughout this process, the battery's state of charge (SOC) is maintained



between its minimum and maximum levels. In the condition without PV, all power is supplied by the grid.

### Case 2:

This case has been analyzed under two conditions: one with PV and one without PV. Here, the EV's battery bank acts as an intermediary energy storage stage. During the daytime, PV energy is used to meet the load demands of the household and the EV battery bank. If PV energy is insufficient to meet the load demand, the remaining energy is supplied by the grid. At night, when PV energy is unavailable, the battery serves as the energy source for household demands. If the battery bank's discharge voltage exceeds a certain threshold, it is recharged using grid power while also supplying energy to the home. The charging and discharging schedule of the battery bank is intelligently optimized to minimize energy expenses. To achieve this optimal solution, a smart home energy management system with a charge controller is seamlessly integrated into the setup. In the condition without PV, all power is supplied by the grid.

### Case 3:

In this scenario, the EV battery bank serves as an additional energy source to meet energy requirements and reduce energy expenses. The home primarily relies on PV and grid power to meet its energy needs. However, energy is also directed from the home's system to the EV battery bank through a home energy management system equipped with a charge controller. Once the EV battery bank is charged, it functions as an extra energy reservoir, supplementing the home's energy demands and thereby lowering overall energy costs. The schedule for charging and discharging the battery bank is strategically optimized to minimize energy expenses. In the condition without PV, all power is supplied by the grid.

## 2.1 Sine Cosine Algorithm (SCA)

The most recent advancement in the realm of algorithms influenced by nature is the SCA [24]. The sine and cosine functions' properties are used in SCA to find the optimal solution. Initially, a random integer  $r \sim U(0, 1)$  is produced in order to update the search agents in SCA. If  $r < 0.5$ , the following equations are then executed:

Table 1: Parameter details for algorithms

Algorithm	Parameter	Value of the parameter
SCA	$r_1$	$a_o = \left(1 - \frac{t}{T}\right), a_o = 2$
	$r_2$	$2 \cdot \pi \cdot r$ where $r = \text{rand}()$
	$r_3$	$2 \cdot r$ where $r = \text{rand}()$



PSO	$c_1$	2.0
	$c_2$	2.0
GWO	$a$	$a_o = \left(1 - \frac{t}{T}\right), a_o = 2$
	$C$	$2 * .r$ where $r = \text{rand}()$
SC-GWO	$w$	$0.7 - 0,5\left(\frac{t}{T}\right)$
	$r_1$	$\text{rand}()$
	$r_2$	$\text{rand}()$

where  $x_{i,j}^{t+1}$  and  $x_{i,j}^t$  represent the positions of  $i$ th solution vector (search agents) in  $j$ th dimension at iterations  $t + 1$  and  $t$ , respectively.  $x_b$  is the best available solution in the population.  $r_1$  is a random number that decides the area for exploration or exploitation. The random number  $r_1$  is taken as linearly decreasing variable from the value 2 to 0. The random number  $r_2$  decides the random movement of search agent but either in the direction of the best solution  $x_b$  or outwards direction of the best solution. The parameter selection that has been fixed in the original SCA is presented in Table 1.

where the locations of the  $i$ th solution vector (search agents) in the  $j$ th dimension at iterations  $t + 1$  and  $t$ , respectively, are represented by the variables  $x_{i,j}^{t+1}$  and  $x_{i,j}^t$ . Among the people,  $x_b$  is the top option. An arbitrary integer,  $r_1$ , determines the region to be explored or exploited. Assuming a linearly declining variable from value 2 to 0, the random number  $r_1$  is used. The search agent moves randomly, either in the direction of the best answer ( $x_b$ ) or outward from it, depending on the random integer  $r_2$ . Table 1 displays the parameter selection that was fixed in the initial SCA.

By expanding the range of the sine and cosine functions to  $[-2, 2]$ , the exploration in the SCA is accomplished. By multiplying the sine and cosine functions by a factor of  $r_1$ , this range is achieved. The exploitation and exploration inside the algorithm is ensured by the search agents' repositioning, either toward or away from the optimal solution.

In order to conduct a better search, any optimization algorithm must strike a proper balance between exploration and exploitation. In the SCA, this balance is achieved by the random variable  $r_1$ , which permits high exploration in the early algorithm iterations and exploits the found promising search areas in the later iterations. The method iterates as follows, decreasing the random number  $r_1$  each time:



$$x_{i,j}^{t+1} = x_{i,j}^t + r_1 \cdot \sin(r_2) \cdot |r_3 x_b^t - x_{i,j}^t| \quad (1)$$

$$x_{i,j}^{t+1} = x_{i,j}^t + r_1 \cdot \cos(r_2) \cdot |r_3 x_b^t - x_{i,j}^t| \quad (2)$$

$$r_1 = 2 - 2 \cdot \left(\frac{t}{T}\right) \quad (3)$$

### Algorithm 1: Pseudo code of SCA

- 1 Set the search agents to start
- 2 Apply the objective function to each search agent's evaluation.
- 3 From the list of search agents, choose the optimal solution  $x_b$ .
- 4 Set the random parameter  $r_1$  and the iteration count  $t = 0$
- 5 while  $t < T$
- 6     For every search engine
- 7     Equations (1-3) are used to update the search agent's position using the solution
- 8     Examine the most recent version of the search engine
- 9     Update the optimal  $x_b$  solution.
- 10    Modify the  $r_1$ ,  $r_2$ , and  $r_3$  settings.
- 11  $t = t + 1$
- 12 end
- 13 Provide the optimal response,  $x_b$ .

## 2.2 Grey Wolf Optimizer (GWO)

Grey wolf optimizer is a leadership hierarchy-based optimization algorithm and was developed by Mirjalili et al. in 2014 [25]. Mirjalili et al. have observed the social and hunting behavior of grey wolves and modeled them into mathematical form to develop an optimization algorithm. In a pack of grey wolves, wolves proceed their search process in three steps, namely tracking, encircling and attacking the prey. In the Grey Wolf Optimizer (GWO), the search process centers on three key search agents referred to as alpha, beta, and delta wolves. These leaders are selected by the entire pack of wolves, considering their dominance and intelligence levels. The formulas employed to adjust the positions of these search agents are as follows:

where  $x_\alpha^t$ ,  $x_\beta^t$  and  $x_\delta^t$  are the states of leaders alpha, beta and delta wolf at  $i$ th iteration, respectively, and  $A$ ,  $A_\alpha$ , and  $A_\beta$  are the random vectors and can be obtained with the help of equations:

$$x_{i,j}^{t+1} = (x_1 + x_2 + x_3) \quad (4)$$

$$x_1 = x_\alpha^t - A_\alpha \cdot D_\alpha \quad (5)$$



$$x_2 = x_\beta^t - A_\beta \cdot D_\beta \quad (6)$$

$$x_3 = x_\delta^t - A_\delta \cdot D_\delta \quad (7)$$

$$A = 2ar_1 - a \quad (8)$$

$$a = 2 - 2 \cdot \left(\frac{t}{T}\right) \quad (9)$$

The difference vectors  $D_\alpha$ ,  $D_\beta$  and  $D_\delta$  can be obtained by the following equations:

$$D_\alpha = |C_\alpha x_\alpha^t - x_{i,j}^t| \quad (10)$$

$$D_\beta = |C_\beta x_\beta^t - x_{i,j}^t| \quad (11)$$

$$D_\delta = |C_\delta x_\delta^t - x_{i,j}^t| \quad (12)$$

$$C = 2r_2 \quad (13)$$

- 1 Establish the gray wolf population.
- 2 Establish the initial values for  $\alpha$  and the maximum number of iterations.
- 3 Determine each grey wolf's level of fitness.
- 4 Choose the leaders for the following roles:
  - 5  $x_\alpha$  (the most suitable answer)
  - 6  $x_\beta$  (the next-best option)
  - 7  $x_\delta$  (third-best solution)
- 8 Set the iteration count  $t=0$ .
- 9 While  $t <$  maximum number of iterations:
  - 10 Equations (4) through (13) may be used to update the positions of each wolf.
  - 11 Determine each grey wolf's level of fitness.
  - 12 Update the wolves that are leading ( $x_\alpha$ ,  $x_\beta$ ,  $x_\delta$ ).
  - 13 Refresh the value of  $\alpha$ .
  - 14 Increment  $t$  by 1.
- 15 End while.
- 16 Return the best solution.

### 2.3 Previous work on SCA and GWO

Numerous researchers have aimed to enhance the Sine Cosine Algorithm (SCA) to boost its search efficiency. For example, one study proposed a modified SCA leveraging orthogonal parallel information [26], while another employed opposition-based learning to accelerate convergence [27]. A different approach addressed the high exploration tendency in SCA's search mechanism [28]. The combination of an Extreme Learning Machine with a



modified SCA was explored for pathological brain detection [29], and a hybrid approach combined Water Wave Optimization with SCA to enhance global optimization [30]. Additionally, SCA has been integrated with Differential Evolution (DE) for visual tracking [31], and Q-learning was incorporated with a sine-cosine strategy to tackle combinatorial problems [32]. An orthogonal learning-driven multi-swarm SCA was proposed to enhance both global exploration and local exploitation [33]. Moreover, SCA has been hybridized with the Artificial Bee Colony (ABC) algorithm and simulated quenching to balance exploration and exploitation [34].

Similarly, the Grey Wolf Optimizer (GWO) faces issues like stagnation at sub-optimal solutions and premature convergence. Enhancements to GWO have been proposed to improve its search efficiency. For instance, an Improved GWO (IGWO) was developed for training q-Gaussian radial basis function neural networks [35], and GWO was hybridized with crossover and mutation operators for economic dispatch problems [36]. Fuzzy hierarchical operators were introduced to create modified GWO versions [37], and fuzzy logic has been utilized to enhance search quality and parameter adaptation. GWO has been applied to modular granular neural networks for human recognition [38], and hybridized with the Genetic Algorithm (GA) to minimize molecular potential energy [39]. Concepts like random walk were incorporated to improve the leadership dynamics of the grey wolf pack [40, 41], and a Cauchy operator was used to enhance searchability [41]. A new position update equation was proposed to improve GWO's exploration capabilities [42], and opposition-based learning along with chaotic maps have been employed to increase convergence speed and local exploitation [43].

In another study [44], a hybrid algorithm combining SCA and GWO, known as HGWOSCA, was proposed to leverage GWO's exploitation strength and SCA's exploration strength, using the SCA search equation to update only the best solution (alpha wolf). Building on the NFL theorem's principle of improving algorithmic search efficiency, this paper introduces a hybrid algorithm, SC-GWO. The SC-GWO algorithm enhances SCA's exploration capabilities initially and then balances exploitation and exploration through hybridization with GWO. This hybrid algorithm is structurally distinct from HGWOSCA. The detailed description of the SC-GWO algorithm is provided in the following sections.

## 2.4 Proposed SC-GWO Algorithm

This section first discusses the motivation behind hybridizing SCA and GWO, followed by presenting the framework of the proposed algorithm and its pseudo-code.

### 2.4.1 Motivation

While SCA is highly regarded for its strong exploration capabilities, it sometimes struggles with low exploitation and an imbalanced approach between exploration and exploitation. SCA's propensity to bypass correct solutions during its search can lead to weak local



searchability. On the other hand, GWO successfully balances exploration and exploitation but can become stagnant at local optima, particularly when many local optima exist. To address these challenges, the new SC-GWO method is introduced. In SC-GWO, the search mechanism of SCA is first modified based on social and cognitive components. This enhanced search mechanism is then combined with GWO to achieve a more effective balance between exploitation and exploration. The following section provides a detailed description of the proposed SC-GWO algorithm.

### 2.4.2 SC-GWO Algorithm

The SC-GWO algorithm enhances the original SCA by introducing three significant features: (1) the inclusion of social and cognitive directional components, (2) the application of a weighted factor to the position component, derived from SCA's distinctive search mechanism, to ensure a balance of diversity, and (3) the incorporation of the GWO phase to achieve an optimal balance between exploration and exploitation. The following subsections will provide a detailed explanation of these enhancements.

### 2.4.3 Social and Cognitive Components

In the SC-GWO algorithm, the search equation incorporates social and cognitive components. This inclusion ensures that every search agent contributes to the process and investigates promising areas close to the best memories of the search agents. These components constrain the search agents around their personal best and the global best memories, facilitating the exploitation of promising regions near the top available memories.

### 2.4.5 The Weighted Factor for the Position Component of SCA

In SC-GWO, a weighted factor is introduced for the position component obtained by SCA's original search mechanism. This factor controls high diversity during the search, preventing the skipping of true solutions. The modified search equations based on these features are as follows:

$$x_{i,j}^{t+1} = w \cdot x_{i,j}^{t+1} + r_1 \cdot (x_{ip,j}^t - x_{i,j}^t) + r_2 \cdot (x_{b,j}^t - x_{i,j}^t) \quad (14)$$

where  $w$  is a weight factor that controls diversity during the search. In the algorithm, it has been fixed in the interval  $[0.7, 0.2]$  and decreased linearly over the iterations.  $r_1$  and  $r_2$  are the uniformly distributed random numbers between 0 and 1.  $x_{ip}^t$  and  $x_b^t$  represented the personal best position of  $i$  th candidate solution and global best solutions at  $t$  th iteration, respectively, and  $x_i^{t+1}$  is the updated position of the candidate solution  $x_i$  at iteration,  $t + 1$  using original SCA.



## 2.4.6 Integration of GWO Phase

In the SC-GWO algorithm, new promising regions are explored using the original SCA along with the proposed factors, after which each search agent undergoes the GWO phase. This phase ensures a balanced approach between exploration and exploitation throughout the search process. Additionally, the GWO phase allows for search operations to be concentrated around the best solutions, leveraging the optimal memory of the population. During the GWO phases, search agents, initially dispersed to investigate new areas of the search space, update their positions based on the best solutions within the population, thereby finding new optimal positions.

The search procedure of the proposed SC-GWO algorithm is presented in Algorithm 3.

```
1  Configure the following parameters: maximum number of iterations (T), population size (NP).
2  Set up the population of search agents,  $P = [x_{i,j}]$  from scratch
3  Determine the fitness level for every search agent.
4  Initialize the inertia weight  $w$ 
5  Out of all the search agents, choose the best answer ( $x_b$ )
6  Set the loop counter  $it = 0$ 
7  while  $it < T$ 
8      Update the weight of inertia  $w$ 
9      for  $i = 1:NP$ 
10         update the position of each search agent using equation (1), (2) and (14)
11         calculate the fitness of updated search agent  $x'_i$ 
12         update the personal best solution  $x_{ip}$ 
13     end of for
14     select the three best solutions as alpha, beta and delta from the set
15      $\{x_b\} \cup P'$  for GWO phase, where  $P' = [x'_{i,j}]$ 
16     Set  $P = P'$ 
17     %%%%%%%%%% GWO phase %%%%%%%%%%
18     for  $i = 1:NP$ 
19         update the position of search agent  $x_i$  using equation (4)
20         calculate the fitness at updated search agent  $x'_i$ 
21         update the personal best solution  $x_{ip}$ 
22     end of for
23     update the best solution  $x_b$ 
24      $P = [x'_{i,j}]$ 
25      $it = it + 1$ 
26 end of while
27 return the best solution  $x_b$ 
```



$$\sum(C_{total}(t)=(P_{load}(t)-\{P_{PV}(t)+S(t)\times P_{EV-charge}(t)\})\times C_{e-off-peak}+P_{load}(t)\times C_{e-peak}(t)) \quad (15)$$

$$\sum(C_{total}(t)=(P_{load}(t)-\{P_{PV}(t)+S(t)\times P_{EV-charge}(t)\})\times C_{e-off-peak}+[P_{load}(t)-S(t)\times(P_{load}(t)-P_{threshold})]\times C_{e-peak}(t)) \quad (16)$$

### Explanation:

1.  $P_{PV}(t)$ : This represents the power generated by the PV system at time  $t$ . It is subtracted from the load  $P_{load}(t)$  because the PV energy offsets the amount of electricity that needs to be drawn from the grid.
2. **Updated Terms:**
  - $P_{load}(t)$ : Total residential load at time  $t$ .
  - $S(t)$ : Status of the EV charging (1 if charging, 0 otherwise).
  - $P_{EV-charge}(t)$ : Power used for EV charging at time  $t$ .
  - $C_{e-off-peak}$ : Cost of electricity per kWh during off-peak hours.
  - $C_{e-peak}(t)$ : Cost of electricity per kWh during peak hours.
  - $P_{threshold}$ : Planned peak load reduction threshold.
  - $C_{total}(t)$  : Total cost

### 2.4.7 PV design

Photovoltaic (PV) cells transform sunlight (photons) into electrical power via the photovoltaic effect. To achieve the desired current and voltage at the output of a PV panel, PV cells are connected in series and/or parallel configurations. The relationship between the current ( $I$ ) and voltage ( $V$ ) of a PV cell is given by Equation (17).

$$I_{pv} = I_{pc} - I_s \exp\left(\frac{q(V_{pv}+I_{pv}R_{se})}{N_s n k T}\right) - 1 - \frac{V_{pv}-I_{pv}R_{se}}{R_{sh}} \quad (17)$$

In this context,  $I_{pc}$  represents the photovoltaic current (A),  $I_s$  is the cell's reverse saturation current (A),  $q$  denotes the electron charge ( $1.602 \times 10^{-19}$  C),  $n$  is the cell's ideality factor,  $k$  is the Boltzmann constant ( $1.381 \times 10^{-23}$  J/K),  $T$  is the operating temperature (K),  $N_s$  indicates the number of PV cells connected in series,  $R_{se}$  is the series resistance of the cell ( $\Omega$ ), and  $R_{sh}$  is the shunt resistance of the cell ( $\Omega$ ).

The sizing of a photovoltaic system can be determined using Equation (18).



$$PV\text{size} = \frac{L_d}{I_{dd}(\text{kWh})} \quad (18)$$

Here,  $L_d$  is the load to be supplied by the PV generation (kWh),  $I_{dd}$  refers to the peak sun hours, which is approximately 5.7 hours per day in the target area, and  $d$  is the de-rating factor, assumed to be 85%.

#### 2.4.8 EV design

In recent years, lithium-ion (Li-ion) batteries have gained widespread use in hybrid electric vehicles (HEVs) and electric vehicles (EVs) because of their high specific energy, high energy density, low self-discharge rate, safety, excellent charge and discharge rates, and long lifespan compared to other battery types. Consequently, this study utilizes a Chevrolet Spark EV, which is equipped with a Li-ion battery. The battery can be modeled using Equation (19).

In this model,  $V_{batt}$  denotes the terminal voltage of the battery (V),  $V_{oc}$  represents the open-circuit voltage (V),  $R_i$  is the internal resistance ( $\Omega$ ),  $i_{batt}$  is the actual load current of the battery (A)—negative during charging and positive during discharging—and  $V_D$  is the voltage drop due to the polarization process (V), also known as the polarization voltage.

The state of charge (SOC) of the battery, expressed as a percentage, can be determined using Equation (20), known as the ampere-hour integral or Coulomb counting method. In this equation,  $SOC_0$  is the initial state of charge (%),  $C_N$  is the rated capacity (Ah), and  $\eta$  represents the Coulomb efficiency.

The SOC will vary based on charging from the grid and PV or discharging to supply the load, according to the constraints of the EV battery capacity. The SOC can be further defined using Equation (21). Here,  $(SOC(t))$  is the state of charge at time  $t$ ,  $I_{PVEV}(t)$  is the current from PV to vehicle,  $I_{GEV}(t)$  is the current from grid to vehicle, and  $I_{EVL}(t)$  is the current from vehicle to load.

To prolong the battery's lifespan by minimizing deep charge/discharge cycles, a minimum and maximum limit for the SOC is established. This is done to avoid overcharging or deep discharging of the EV battery. The SOC is thus constrained by the limits defined in Equation (22), where  $SOC_{min}$  and  $SOC_{max}$  are the minimum and maximum state of charge limits, respectively.

$$V_{batt} = V_{oc} - R_i i_{batt} - V_D \quad (19)$$

$$SOC = SOC_0 - \frac{1}{C_N} \int_{t_0}^t h_i i_{batt} dt \quad (20)$$



$$SOC(t) = \begin{cases} SOC_0 + \frac{1}{C_N} \int_{t_0}^t h(I_{PV}E_V(t) + I_{GEV}(t))dt & \text{if charging} \\ SOC_0 - \frac{1}{C_N} \int_{t_0}^t hI_{EVL}(t)dt & \text{if discharging} \end{cases} \quad (21)$$

$$SOC_{min} \leq SOC(t) \leq SOC_{max} \quad (22)$$

### 2.4.9 Load

To study the different cases a typical load profile has been considered. The Fig. 3 has been used for load profile in the analysis process.

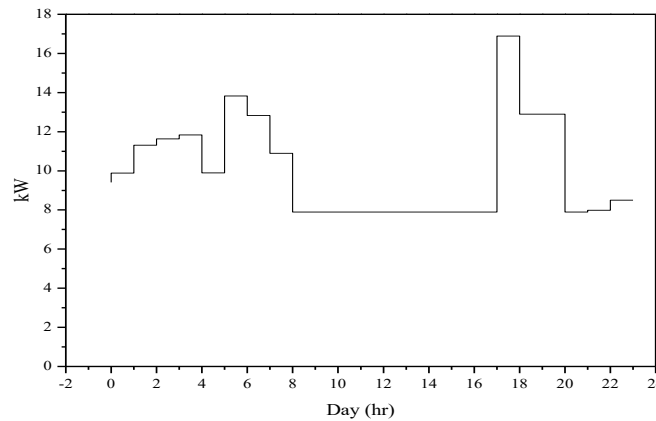


Fig 3. Load profile of the study

## 3. Results and analysis

### 3.1 Without PV

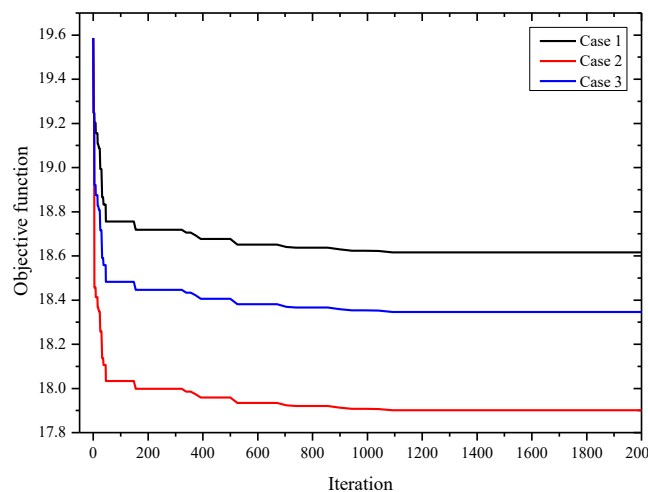


Fig 3: Iteration for cost optimization



The figure shows the objective function values over iterations for three cases: Case 1 (black), Case 2 (red), and Case 3 (blue). Initially, all cases start around 19.6, with a rapid decrease indicating quick early improvement. Case 2 (red) decreases the fastest, stabilizing around 17.90, showing the best performance. Case 3 (blue) decreases more gradually, stabilizing around 18.34, indicating moderate performance. Case 1 (black) decreases initially but stabilizes around 18.61, indicating the least effective performance. The convergence patterns show different efficiency levels, with Case 2 being the most effective, followed by Case 3 and then Case 1. All cases eventually reach stable values, demonstrating convergence. The variations in final objective function values suggest that different methods or parameters were used, affecting their performance.

### 3.1.1 Battery analysis

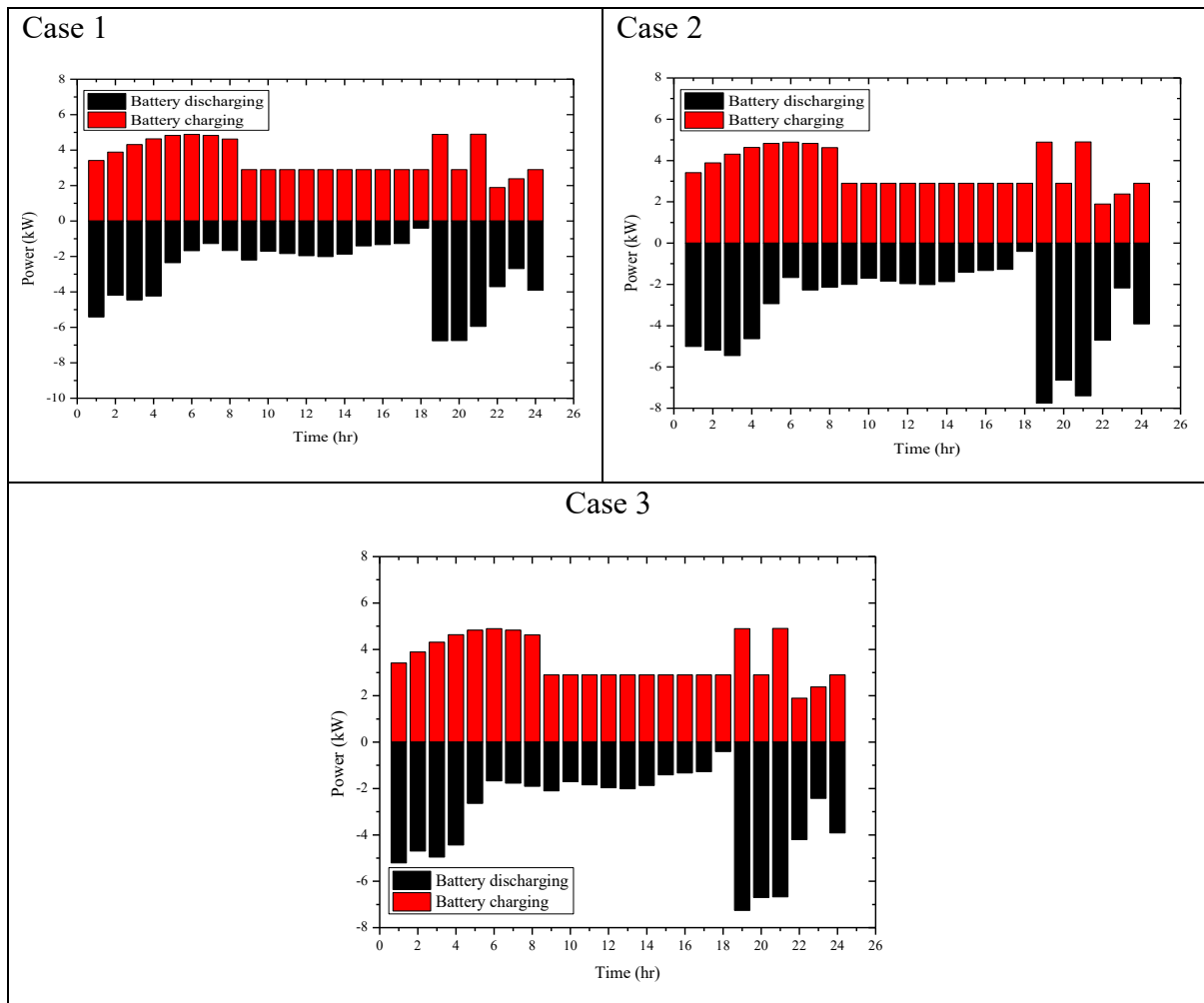


Fig 4: Battery charging and discharging

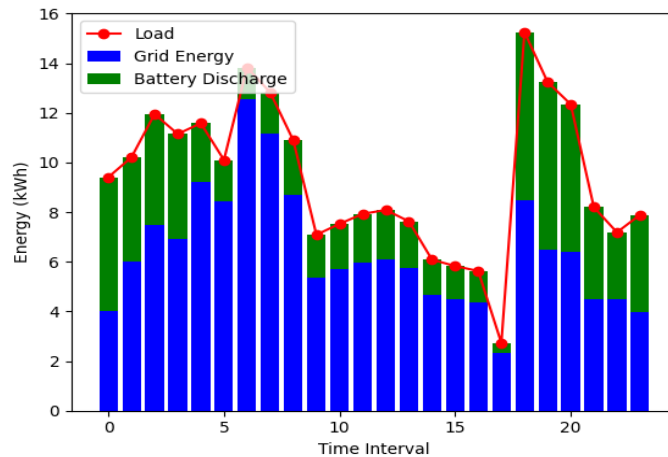


The graphical representation in Fig.4 illustrates the temporal patterns of battery charging and discharging power. Analysis of the figure reveals distinctive trends among the different cases. Notably, Case 2 exhibits the highest total battery discharging power. Conversely, Case 1 demonstrates the lowest total battery discharging power.

In summary, the graphical depiction offers valuable insights into the distinct charging and discharging power profiles of the various cases. It highlights the dynamic interplay between energy sources and loads, showcasing the efficacy of each case's energy management strategy.

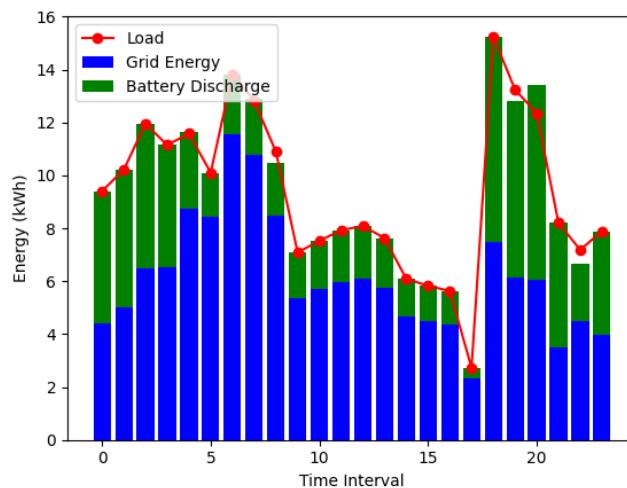
### 3.1.2 Energy analysis

#### Case 1



(a) Case 1

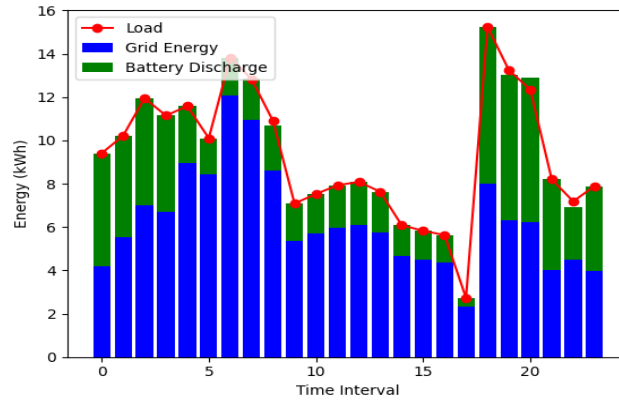
#### Case 2



(b) Case 2



### Case 3



(c) Case 3

Fig 5: Energy demand of the system

The figures Fig 5: (a-c) illustrate the distribution of energy usage over a series of time intervals for three different cases. The red line with circular markers represents the load (demand) in kW, while the stacked bars show the energy sources meeting this load. The blue segments of the bars represent energy drawn from the grid, and the green segments represent energy supplied by battery discharge. Initially, both the grid energy and battery discharge contribute to meeting the load, with the total closely following the red load line. Noticeably, at certain intervals, the battery discharge contributes significantly, reducing reliance on grid energy. Conversely, during the period when the load decreases sharply, leading to a minimal battery discharge and a reliance almost entirely on grid energy. Overall, the combined energy from the grid and battery consistently meets or exceeds the load, ensuring no shortfall in energy supply.

### 3.2 With PV

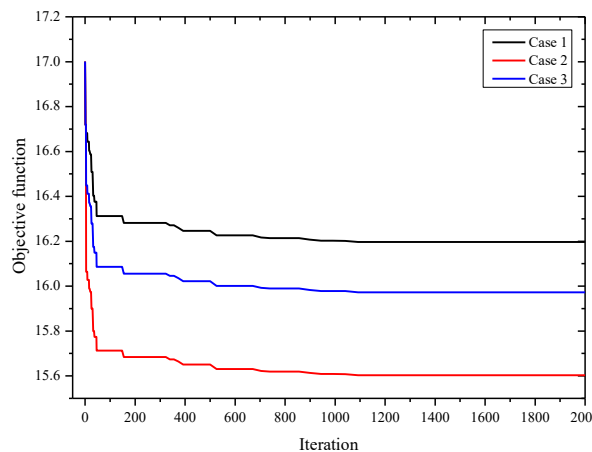


Fig 6: Iteration for cost optimization



The figure 6 illustrates the objective function values over iterations for three cases. Case 1 begins near 17.0, decreases rapidly, and stabilizes just above 16.1965. Case 2 also starts around 17.0, drops the fastest, and stabilizes at the lowest value, approximately 15.6. Case 3 (blue line) starts slightly below 17, decreases gradually, and stabilizes around 15.97, the highest final value among the cases. All cases show an initial rapid decline, indicating quick improvement, followed by convergence to stable values. Case 2 achieves the lowest objective function value, suggesting it is the most efficient, while Case 3 has the highest stabilized value, indicating it is the least effective. The differences in final values imply varying efficiencies and effectiveness of the strategies or parameters used in each case, with Case 2 being the most optimal and Case 3 the least.

### 3.2.1 Battery energy

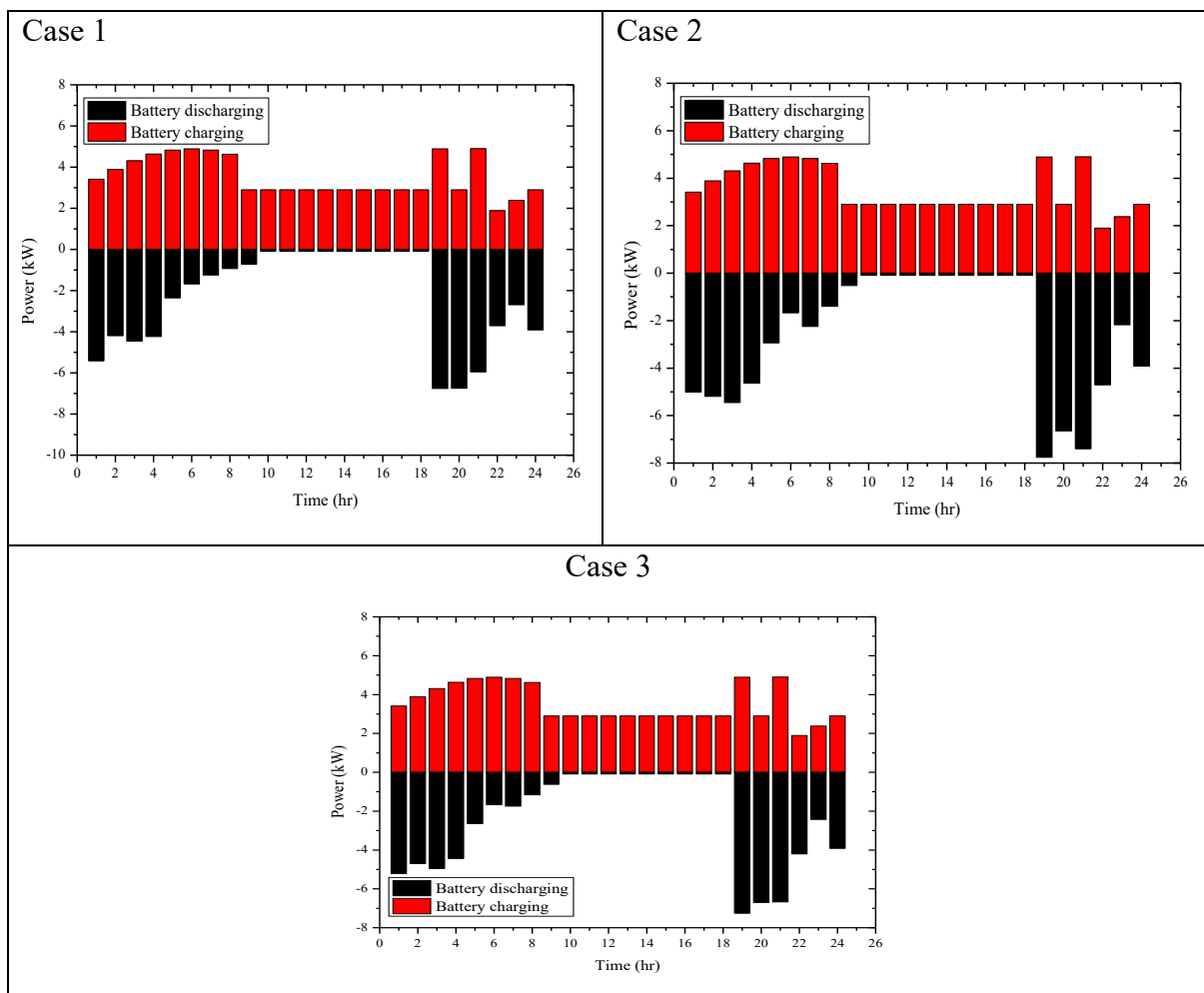


Fig 7: Battery charging and discharging

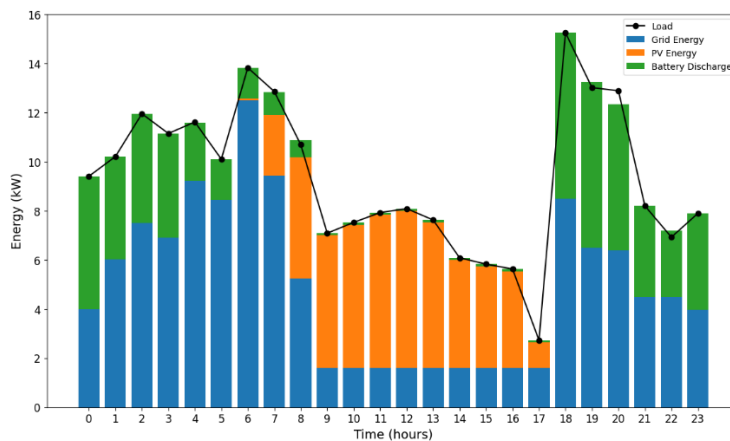
The figure 7 illustrate the battery charging and discharging patterns over a 24-hour period. In three graphs, battery charging (red bars) predominantly occurs during the middle of the day (6



to 17 hours) when there is likely excess energy from sources like solar PV. Battery discharging (black bars) happens mostly during the 0 to 6 hours and 17 to 24 hours when the energy demand is higher, and solar energy is not available. The intensity of charging and discharging varies slightly between the three figures, with the second graph showing a more pronounced discharge during the 17 to 22 hours and a slightly higher charging rate during midday 11 to 14 hours. This indicates a strategic utilization of battery storage to balance energy supply and demand, ensuring availability during peak demand periods and charging during periods of low demand or high renewable energy production.

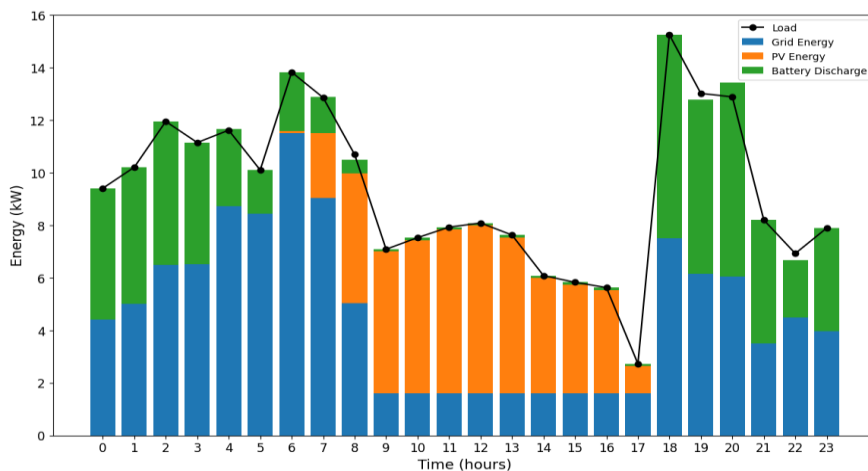
### 3.2.2 Energy Analysis

#### Case 1



(a) Case1

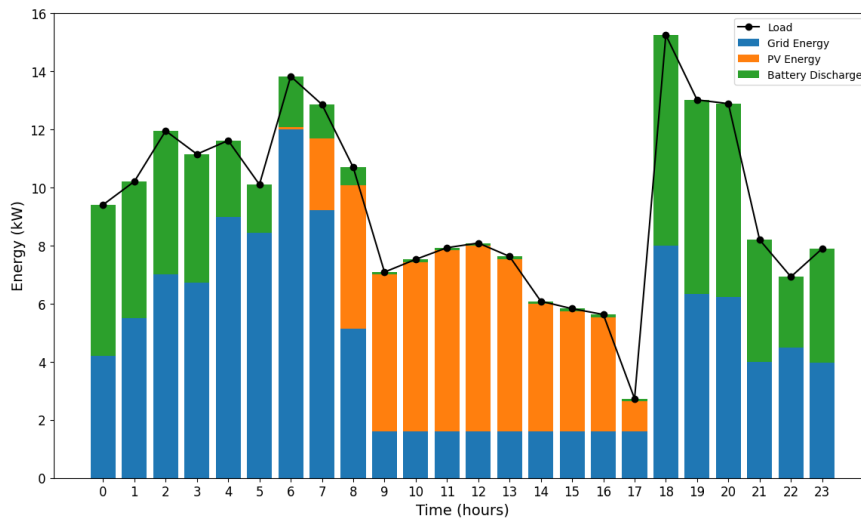
#### Case 2



(b) Case 2



## Case 3



(c) Case 3

Fig 8: Energy demand of the system

The analysis of the figures 8 (a-c) presents two scenarios depicting energy consumption and sources in a residential setting across a 24-hour period. Case 1 showcases predominant grid energy usage in the early hours, gradually supplemented by PV energy and intermittently by battery discharge. As daylight progresses, PV energy becomes the primary source, reducing grid reliance until sunset, where grid usage increases again. Case 2 mirrors this pattern but with a more optimized use of PV energy, resulting in a slightly more balanced load distribution. Both cases effectively utilize battery discharge during peak load times and when PV energy is insufficient, thereby reducing grid dependency. Overall, the integration of PV systems and battery storage demonstrates a clear reduction in grid energy consumption during daylight hours, with strategic battery usage further enhancing energy management, particularly during peak demand and PV energy absence. Case 3 figure illustrates a 24-hour energy distribution involving Load, Grid Energy, PV Energy, and Battery Discharge. The energy demand (Load) is highest in the early morning and evening, peaking at hours 6 and 18. Grid Energy (blue bars) dominates during the night and early morning (0-7 hours) and again in the 17-23 hours. PV Energy (orange bars) starts contributing from hour 6, peaks between hours 9 and 15, and is absent during the night. Battery Discharge (green bars) supplements energy in the 5-7 hours and 18-21 hours, with minimal use midday. The graph shows a strategic use of solar energy during daylight and a mix of grid energy and battery discharge to meet demand during other periods.



### 3.3 Cost comparison

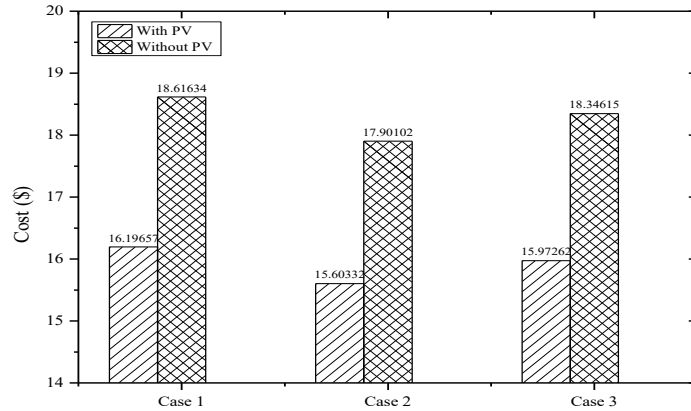


Fig 9: Cost comparison

The Fig 9 illustrates a cost comparison across three cases, each evaluated with and without photovoltaic (PV) systems. In Case 1, costs drop from approximately \$18.61 without PV to \$16.19 with PV, saving around \$2.42. For Case 2, costs decrease from \$17.90 without PV to \$15.60 with PV, resulting in a \$2.30 saving. In Case 3, costs reduce from \$18.34 without PV to \$15.97 with PV, saving about \$2.37. These analyses highlight the effectiveness of PV systems in reducing energy expenses. Overall, integrating PV systems markedly decreases costs across all cases. Case 1 has the highest cost without PV, followed by Case 3 and Case 2. With PV, costs are lowest in Case 2, followed by Case 3 and Case 1. The findings clearly support PV technology as a cost-effective solution for energy management in residential settings, emphasizing significant cost reductions when PV systems are utilized.

### 3.4 Battery power comparison

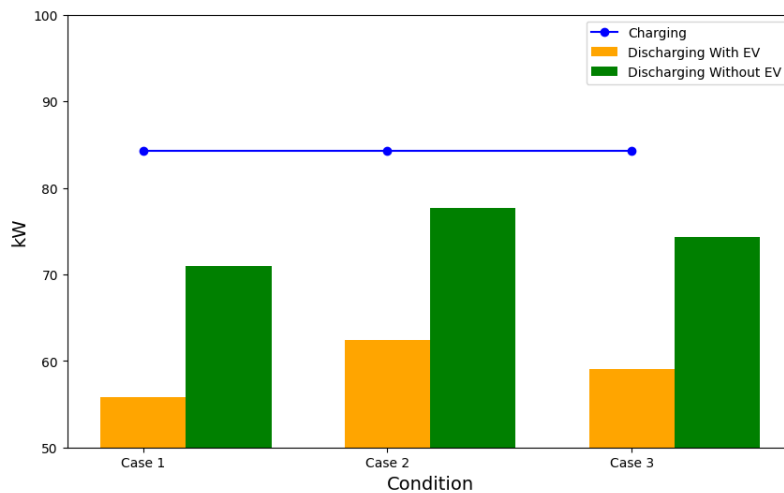


Fig 10. Battery energy



The Fig 10 reveals that all cases have identical charging values of 84.24268 kW, indicating that the battery storage capacity is consistent across all scenarios. However, the discharging values, both with and without EVs, vary. Case 2 exhibits the highest discharging values (62.4497 kW with EV and 77.69965 kW without EV), while Case 1 shows the lowest (55.7683 kW with EV and 71.01802 kW without EV). This suggests that, although the storage capacity is the same, Case 2 has higher energy utilization, implying more effective energy management system.

#### 4. Conclusion

the pressing global challenges of fossil fuel scarcity and environmental degradation have spurred the development of renewable energy technologies and electric vehicles (EVs) to alleviate dependence on traditional energy sources and mitigate pollution. However, integrating these technologies into existing infrastructure poses significant challenges, including grid instability due to the intermittent nature of renewables and erratic EV charging behaviors. Addressing these issues necessitates sophisticated energy management systems that synchronize EV charging with renewable energy generation. This study proposes an innovative energy management strategy for smart homes equipped with both PV systems and EVs. The strategy employs a two-stage monitoring system activated by various criteria to optimize energy flow and minimize costs while meeting power demands and maintaining EV battery state-of-charge (SOC). Results demonstrate the effectiveness of the proposed strategy, with Case 2 exhibiting the most efficient performance in both scenarios, followed by Case 3 and then Case 1. Battery analysis reveals distinct charging and discharging patterns among the cases, with Case 2 demonstrating the highest total battery discharging power and Case 1 exhibiting the lowest. Energy analysis illustrates strategic utilization of battery storage to balance energy supply and demand, reduce grid dependency, and optimize PV energy utilization, particularly during peak demand periods. Cost comparison demonstrates significant savings with PV integration across all cases, underscoring the cost-effectiveness of PV systems for residential energy management. Integrating PV technology markedly reduces energy expenses, with Case 2 showcasing the most substantial cost reduction both with and without PV, followed by Case 3 and then Case 1. These findings underscore the viability of PV systems as a cost-effective solution for residential energy management, offering substantial savings and contributing to grid stability and environmental sustainability. Looking ahead, future research endeavors could explore enhanced algorithms and advanced technologies to further optimize energy scheduling and maximize cost savings. Additionally, there is scope for investigating the scalability and interoperability of such energy management systems within larger smart grid frameworks. Overall, by continuing to innovate in energy management strategies and fostering synergies between renewable energy, EVs, and smart grid technologies, we can pave the way for a more sustainable and resilient energy future.



## Reference

1. K. Liu, Q. Wang, Z. Luo, X. Zhao, S. Su, and X. Zhang, "Planning Mechanism Design and Benefit Analysis of Electric Energy Substitution: A Case Study of Tobacco Industry in Yunnan Province, China," *IEEE Access*, vol. 8, pp. 12867–12883, 2020, doi: 10.1109/ACCESS.2020.2966176.
2. D. A. Savio, V. A. Juliet, B. Chokkalingam, S. Padmanaban, J. B. Holm-Nielsen, and F. Blaabjerg, "Photovoltaic integrated hybrid microgrid structured electric vehicle charging station and its energy management approach," *Energies*, vol. 12, no. 168, 2019, doi: 10.3390/en12010168.
3. S. R. Sinsel, R. L. Rienke, and V. H. Hoffmann, "Challenges and solution technologies for the integration of variable renewable energy sources—A review," *Renew. Energy*, vol. 145, pp. 2271–2285, 2020, doi: 10.1016/j.renene.2019.07.008.
4. T. Kemmler and B. Thomas, "Design of Heat-Pump Systems for Single-and Multi-Family Houses using a Heuristic Scheduling for the Optimization of PV Self-Consumption," *Energies*, vol. 13, no. 1118, 2020, doi: 10.3390/en13051118.
5. N. O. Kapustin and D. A. Grushevenko, "Long-term electric vehicles outlook and their potential impact on electric grid," *Energy Policy*, vol. 137, no. 111103, 2020, doi: 10.1016/j.enpol.2019.111103.
6. R. Luthander, M. Shepero, J. Munkhammar, and J. Widen, "Photovoltaics and opportunistic electric vehicle charging in the power system—A case study on a Swedish distribution grid," *IET Renew. Power Gener.*, vol. 13, pp. 710–716, 2019, doi: 10.1049/iet-rpg.2018.5514.
7. Y. M. Wi, J. U. Lee, and S. K. Joo, "Electric vehicle charging method for smart homes/buildings with a photovoltaic system," *IEEE Trans. Consum. Electron.*, vol. 59, pp. 323–328, 2013, doi: 10.1109/TCE.2013.6490254.
8. B. Tarroja, J. D. Eichman, L. Zhang, T. M. Brown, and S. Samuelson, "The effectiveness of plug-in hybrid electric vehicles and renewable power in support of holistic environmental goals: Part 2-Design and operation implications for load-balancing resources on the electric grid," *J. Power Sources*, vol. 278, pp. 782–793, 2015, doi: 10.1016/j.jpowsour.2014.12.113.
9. G. S. Lakshmi, O. Rubanenko, and I. Hunko, "Renewable Energy Generation and Impacts on E-Mobility," *J. Phys.: Conf. Ser.*, vol. 1457, no. 012009, 2019, doi: 10.1088/1742-6596/1457/1/012009.
10. H. Daki, A. El Hannani, A. Aqqal, A. Haidine, and A. Dahbi, "Big Data management in smart grid: Concepts, requirements and implementation," *J. Big Data*, vol. 4, pp. 1–19, 2017, doi: 10.1186/s40537-017-0070-y.



11. M. Shakeri et al., "An intelligent system architecture in home energy management systems (HEMS) for efficient demand response in smart grid," *Energy Build.*, vol. 138, pp. 154–164, 2017, doi: 10.1016/j.enbuild.2017.01.098.
12. J. Leitao, P. Gil, B. Ribeiro, and A. Cardoso, "A survey on home energy management," *IEEE Access*, vol. 8, pp. 5699–5722, 2020, doi: 10.1109/ACCESS.2020.2964518.
13. D. J. Olsen, M. R. Sarker, and M. A. Ortega-Vazquez, "Optimal penetration of home energy management systems in distribution networks considering transformer aging," *IEEE Trans. Smart Grid*, vol. 9, pp. 3330–3340, 2016, doi: 10.1109/TSG.2016.2626467.
14. F. Luo, G. Ranzi, W. Kong, Z. Y. Dong, and F. Wang, "Coordinated residential energy resource scheduling with vehicle-to-home and high photovoltaic penetrations," *IET Renew. Power Gener.*, vol. 12, pp. 625–632, 2018, doi: 10.1049/iet-rpg.2017.0173.
15. U. Datta, A. Kalam, and J. Shi, "Electric vehicle (EV) in home energy management to reduce daily electricity costs of residential customer," *J. Sci. Ind. Res.*, vol. 77, pp. 559–565, 2018.
16. X. Wu, X. Hu, X. Yin, and S. J. Moura, "Stochastic optimal energy management of smart home with PEV energy storage," *IEEE Trans. Smart Grid*, vol. 9, pp. 2065–2075, 2016, doi: 10.1109/TSG.2016.2582742.
17. S. Khemakhem, M. Rekik, and L. Krichen, "A flexible control strategy of plug-in electric vehicles operating in seven modes for smoothing load power curves in smart grid," *Energy*, vol. 118, pp. 197–208, 2017, doi: 10.1016/j.energy.2016.12.026.
18. S. Khemakhem, M. Rekik, and L. Krichen, "Double layer home energy supervision strategies based on demand response and plug-in electric vehicle control for flattening power load curves in a smart grid," *Energy*, vol. 167, pp. 312–324, 2019, doi: 10.1016/j.energy.2018.11.013.
19. R. Rana, S. Prakash, and S. Mishra, "Energy Management of Electric Vehicle Integrated Home in a Time-of-Day Regime," *IEEE Trans. Transp. Electrif.*, vol. 4, pp. 804–816, 2018, doi: 10.1109/TTE.2018.2855961.
20. O. Erdinc, N. G. Paterakis, T. D. Mendes, A. G. Bakirtzis, and J. P. Catalao, "Smart household operation considering bi-directional EV and ESS utilization by real-time pricing-based DR," *IEEE Trans. Smart Grid*, vol. 6, pp. 1281–1291, 2014, doi: 10.1109/TSG.2014.2371476.
21. X. Wu, X. Hu, S. Moura, X. Yin, and V. Pickert, "Stochastic control of smart home energy management with plug-in electric vehicle battery energy storage and photovoltaic array," *J. Power Sources*, vol. 333, pp. 203–212, 2016, doi: 10.1016/j.jpowsour.2016.09.157.



22. S. Aznavi, P. Fajri, and A. Asrari, "Realistic and intelligent management of connected storage devices in future smart homes considering energy price tag," *IEEE Trans. Ind. Appl.*, vol. 56, pp. 1679–1689, 2019, doi: 10.1109/TIA.2019.2952817.
23. S. Lee and D. H. Choi, "Energy Management of Smart Home with Home Appliances, Energy Storage System and Electric Vehicle: A Hierarchical Deep Reinforcement Learning Approach," *Sensors*, vol. 20, no. 2157, 2020, doi: 10.3390/s20082157.
24. S. Mirjalili, "SCA: a sine cosine algorithm for solving optimization problems," *Knowl-Based System*, vol. 96, pp. 120–133, 2016, doi: 10.1016/j.knosys.2015.12.022.
25. S. Mirjalili, S. M. Mirjalili, and A. Lewis, "Grey wolf optimizer," *Adv. Eng. Softw.*, vol. 69, pp. 46–61, 2014, doi: 10.1016/j.advengsoft.2013.12.007.
26. R. M. Rizk-Allah, "An improved sine–cosine algorithm based on orthogonal parallel information for global optimization," *Soft Comput.*, vol. 23, pp. 7135–7161, 2019, doi: 10.1007/s00500-018-03483-7.
27. M. A. Elaziz, D. Oliva, and S. Xiong, "An improved opposition-based sine cosine algorithm for global optimization," *Expert Syst. Appl.*, vol. 90, pp. 484–500, 2017, doi: 10.1016/j.eswa.2017.08.005.
28. S. Gupta and K. Deep, "Improved sine cosine algorithm with crossover scheme for global optimization," *Knowl-Based Syst*, vol. 165, pp. 374–406, 2019, doi: 10.1016/j.knosys.2018.12.034.
29. D. R. Nayak, R. Dash, B. Majhi, and S. Wang, "Combining extreme learning machine with modified sine cosine algorithm for detection of pathological brain," *Comput. Electr. Eng.*, vol. 68, pp. 366–380, 2018, doi: 10.1016/j.compeleceng.2018.04.020.
30. J. Zhang, Y. Zhou, and Q. Luo, "An improved sine cosine water wave optimization algorithm for global optimization," *J. Intell. Fuzzy Syst.*, vol. 34, pp. 2129–2141, 2018, doi: 10.3233/JIFS-169250.
31. H. Nenavath and R. K. Jatoth, "Hybridizing sine cosine algorithm with differential evolution for global optimization and object tracking," *Appl. Soft Comput.*, vol. 62, pp. 1019–1043, 2018, doi: 10.1016/j.asoc.2017.09.030.
32. K. Z. Zamli, F. Din, B. S. Ahmed, and M. Bures, "A hybrid Q-learning sine-cosine-based strategy for addressing the combinatorial test suite minimization problem," *PLoS ONE*, vol. 13, no. e0195675, 2018, doi: 10.1371/journal.pone.0195675.
33. H. Chen, A. A. Heidari, X. Zhao, L. Zhang, and H. Chen, "Advanced orthogonal learning-driven multi-swarm sine cosine optimization: framework and case studies," *Expert Syst. Appl.*, vol. 144, no. 113113, 2020, doi: 10.1016/j.eswa.2019.113113.



34. S. Gupta and K. Deep, "A novel hybrid sine cosine algorithm for global optimization and its application to train multilayer perceptrons," *Appl. Intell.*, vol. 50, 2019, doi: 10.1007/s10489-019-01570-w.
35. N. Muangkote, K. Sunat, and S. Chiewchanwattana, "An improved grey wolf optimizer for training q-Gaussian Radial Basis Functional-link nets," in *2014 International Computer Science and Engineering Conference (ICSEC)*, 2014, doi: 10.1109/ICSEC.2014.6978223.
36. T. Jayabarathi, T. Raghunathan, B. Adarsh, and P. N. Suganthan, "Economic dispatch using hybrid grey wolf optimizer," *Energy*, vol. 111, pp. 630–641, 2016, doi: 10.1016/j.energy.2016.06.018.
37. L. Rodríguez et al., "A fuzzy hierarchical operator in the grey wolf optimizer algorithm," *Appl. Soft Comput.*, vol. 57, pp. 315–328, 2017, doi: 10.1016/j.asoc.2017.03.043.
38. D. Sánchez, P. Melin, and O. Castillo, "A grey wolf optimizer for modular granular neural networks for human recognition," *Comput. Intell. Neurosci.*, vol. 2017, no. 4180510, 2017, doi: 10.1155/2017/4180510.
39. M. A. Tawhid and A. F. Ali, "A hybrid grey wolf optimizer and genetic algorithm for minimizing potential energy function," *Memetic Comput.*, vol. 9, pp. 347–359, 2017, doi: 10.1007/s12293-017-0247-7.
40. S. Gupta and K. Deep, "Enhanced leadership-inspired grey wolf optimizer for global optimization problems," *Eng. Comput.*, vol. 36, pp. 1–24, 2019, doi: 10.1007/s00366-019-00795-0.
41. S. Gupta and K. Deep, "Cauchy Grey Wolf Optimiser for continuous optimisation problems," *J. Exp. Theor. Artif. Intell.*, vol. 30, pp. 1051–1075, 2018, doi: 10.1080/0952813X.2017.1371232.
42. W. Long, J. Jiao, X. Liang, and M. Tang, "An exploration-enhanced grey wolf optimizer to solve high-dimensional numerical optimization," *Eng. Appl. Artif. Intell.*, vol. 68, pp. 63–80, 2018, doi: 10.1016/j.engappai.2017.10.024.
43. S. Gupta and K. Deep, "An efficient grey wolf optimizer with opposition-based learning and chaotic local search for integer and mixed-integer optimization problems," *Arab. J. Sci. Eng.*, vol. 44, pp. 7277–7296, 2019, doi: 10.1007/s13369-019-04080-x.
44. N. Singh and S. Singh, "A novel hybrid GWO-SCA approach for optimization problems," *Eng. Sci. Technol., an Int. J.*, vol. 20, pp. 1586–1601, 2017, doi: 10.1016/j.jestch.2017.05.001.